Available online at www.sciencedirect.com
SCIENCE DIRECT®
Journal of Organometallic Chemistry 680 (2003) 165–172
Journal of Organometallic Chemistry
www.elsevier.com/locate/jorganchem

Dimesitylborane monomer-dimer equilibrium in solution, and the solid-state structure of the dimer by single crystal neutron and X-ray diffraction

Christopher D. Entwistle [a], Todd B. Marder [a,*], Philip S. Smith [a], Judith A.K. Howard [a], Mark A. Fox [a], Sax A. Mason [b]

[a] *Department of Chemistry, University of Durham, South Road, Durham DH1 3LE, UK*
[b] *Institute Laue Langevin, BP 156, 38042 Grenoble Cedex 9, France*

Received 13 March 2003; received in revised form 1 April 2003; accepted 17 April 2003

Dedicated to Professor M. Frederick Hawthorne on the occasion of his 75th birthday

Abstract

Dimesitylborane dimer has been shown to exist in equilibrium with dimesitylborane monomer in solution. This equilibrium has been investigated by variable concentration and variable temperature multinuclear NMR spectroscopy and values for the dissociation constant, enthalpy and entropy of dissociation were found to be $K_{diss} = (3.2 \pm 0.4) \times 10^{-3}$ M, $\Delta H = 70$ kJ mol^{-1}, and $\Delta S = 212$ J K^{-1}mol^{-1}, respectively. Ab initio methods have been used to investigate the gas-phase structures and energies of both monomer and dimer, and calculated ^{11}B-NMR shifts are also presented. The solid-state structure of dimesitylborane dimer has been investigated by single crystal X-ray diffraction at 100 K and the position of the bridging hydrogen atoms (B–H = 1.340(2), 1.342(2) Å, H–B–H = 92.46(14)°) has been determined accurately, for the first time, by single crystal neutron diffraction at 20 K.

Keywords: Boron; Borane; Equilibrium; X-ray structure; Neutron structure; NMR spectroscopy; Ab initio computations

1. Introduction

Dimesitylborane, first synthesised in 1974 by Hooz et al. [1], is a sterically hindered diarylborane. Its reactivity was investigated by Pelter et al. [2], who found it to be a relatively unreactive borane, reacting only slowly with alkenes at room temperature but rapidly with alkynes, thus allowing the selective monohydroboration of compounds having both alkene and alkyne moieties. In addition, hydroborations are very sensitive to substrate steric effects, as it reacts preferentially with terminal alkenes or alkynes in the presence of disubstituted compounds, with the resulting triorganoboranes having almost exclusively terminal dimesitylboryl groups. The regio- and steriospecificity of dimesitylborane hydroborations has led to its use in the synthesis of air and moisture stable three-coordinate organoboranes and, in particular, the synthesis of conjugated organic materials where the organic π system interacts with the vacant p-orbital situated on boron [3–6]. Hydrolysis is prevented by the sterically demanding mesityl groups, which block the approach of nucleophiles by forming a 'cage' around the vacant p-orbital with their *ortho* methyl groups. Such materials have been shown to have interesting optical and electronic properties, and are promising candidates for use in a wide range of organic electronic devices [3–13].

During our research into the properties of conjugated organic materials containing the dimesitylboryl group, we noticed that the NMR spectra of dimesitylborane always contained minor peaks that did not correspond to dimeric dimesitylborane. Further investigation suggested that in solution, at room temperature, dimesitylborane dimer exists in equilibrium with its monomer.

* Corresponding author. Tel.: +44-191-334-2037; fax: +44-191-384-4737.
E-mail address: todd.marder@durham.ac.uk (T.B. Marder).

0022-328X/03/$ - see front matter
doi:10.1016/S0022-328X(03)00316-4

Although it is generally accepted that diboranes react with unsaturated compounds via a π-complex involving monomeric borane [14], there is little direct experimental evidence to support this, with bis(pentafluorophenyl)borane [15] and 10-trimethylsilyl-9-borabicyclodecane-H [16] being the only other experimentally observed cases of monomer–dimer equilibrium in solution for an organoborane. Monomeric organoboranes are rare, two known examples are the exceptionally hindered di(2,4,6-tri-isopropylphenyl)borane (ditripylborane) [17] and bis(2,3-dimethyl-2-butyl)borane (dithexylborane) [18]. Dioxaborolanes such as catecholborane (HBcat, cat = 1,2-$O_2C_2H_4$), commonly used in hydroborations, are also monomeric [19,20]. We therefore decided to investigate this equilibrium by variable concentration and variable temperature multinuclear NMR spectroscopy. We have also used computational methods to predict the structures, binding energy of the dimer and ^{11}B-NMR chemical shifts of both monomer and dimer, and have reinvestigated the solid-state structure of dimesitylborane (first solved from X-ray data by Power et al. [17]) by X-ray and neutron diffraction. This study represents one of few cases vide infra where neutron diffraction has been used to solve the structure of a compound containing one or more B–H bonds [21,22], and is the only simple diborane (6) compound to have been studied (Scheme 1).

2. Results and discussion

2.1. NMR results

The ^{11}B{^{1}H}-NMR spectrum of dimesitylborane in d_8-toluene or d_6-benzene at room temperature shows two broad peaks corresponding to monomer (73.3 ppm) and dimer (25.9 ppm). Neither of the peaks show any splitting in their ^{11}B-NMR spectrum due to coupling to hydrogen, almost certainly because of the broadness of the peaks, which is attributed to a combination of slow tumbling due to steric bulk (expected to more significant for the dimer than for the monomer), and the presence of the quadrupolar boron nucleus. In the case of the dimesitylborane monomer, these factors are compounded by the fact that the boron atom is three-coordinate. At room temperature, the peak width at half height is ca. 380 Hz (monomer) and 770 Hz (dimer). The broad peak at 50 ppm corresponds to traces of dimesitylborinic acid (Mes_2BOH, $<1\%$) formed by hydrolysis of dimesitylborane by traces of water.

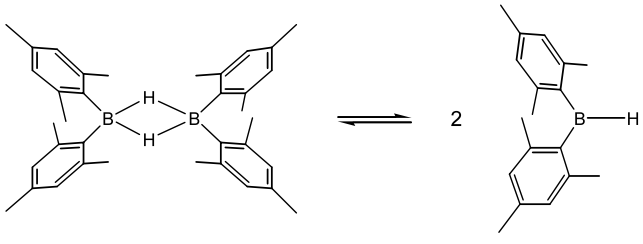

Scheme 1. Schematic reaction mechanism for dimesitylborane dissociation.

In THF solution, the NMR spectrum again shows two peaks, corresponding to monomer and dimer. The dimer peak is shifted upfield by ca. 3 ppm to 22.9 ppm, and the monomer peak is shifted upfield by ca. 8 ppm to 65.1 ppm. This is in contrast to bis(pentafluorophenyl)borane, which forms the isolable complex $(C_6F_5)_2BH\cdot THF$ (^{11}B, $\delta = -1.6$), which is a very weak hydroborating agent [15]. Dimesitylborane may be recrystallised from THF, the resulting solid having no THF present by ^{1}H-NMR, and hydroborations proceed efficiently in THF solution. However, solutions of dimesitylborane in THF have a higher proportion of monomer than those of the same overall concentration of dimesitylborane in aromatic solvents (ca. double the proportion for a 0.1 M solution at ambient temperature), indicating that some stabilisation of the monomer by coordination to THF does occur.

Proton-NMR chemical shifts are presented in Table 1. Without boron decoupling, the monomer B–H peak is not visible and the dimer B–H peak is considerably broadened. The dimer shows evidence of hindered rotation of the mesityl groups, with the aryl-H and *ortho*-methyl-H peaks each giving rise to two singlets; the corresponding groups appear as single peaks in the monomer indicating that reduced steric crowding allows free rotation about the B–C bonds. Though well resolved, the low intensity of the monomer B–H resonance under most conditions precluded its use in calculations. The methyl group region is slightly crowded but the aryl region is well resolved at 500 MHz, so this region was used to quantify the ^{1}H-NMR spectra.

2.2. Variable concentration NMR study

To examine the effect of varying the concentration on the position of the monomer–dimer equilibrium, a series of solutions was prepared by successive dilution and examined by ^{11}B{^{1}H} and ^{1}H{^{11}B}-NMR spectroscopy (Figs. 1 and 2). As the total concentration of dimesitylborane is reduced, the relative concentration of the monomer increases as expected. From this experiment, the ambient temperature dissociation constant, K_{diss}, was calculated from the total concentration of dimesitylborane and the percentage of monomer present in a given solution, and was found to be $(3.2 \pm 0.4) \times 10^{-3}$ M.

Table 1
^{1}H-NMR chemical shifts and relative intensities in C_6D_6 at ambient temperature

	B–H	Aryl	Methyl
Dimer	4.26, s, 2H	6.66, s, 4H; 6.54, s, 4H	2.19, s, 12H; 2.16, s, 12H; 2.01, s, 12H
Monomer	8.17, s, 1H	6.75, s, 4H	2.24, s, 12H; 2.10, s, 6H

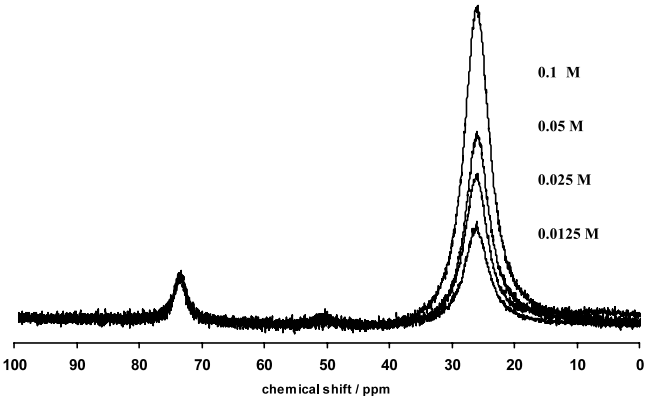

Fig. 1. Effect of varying dimesitylborane concentration on $^{11}B\{^1H\}$ spectra, normalised to monomer intensity.

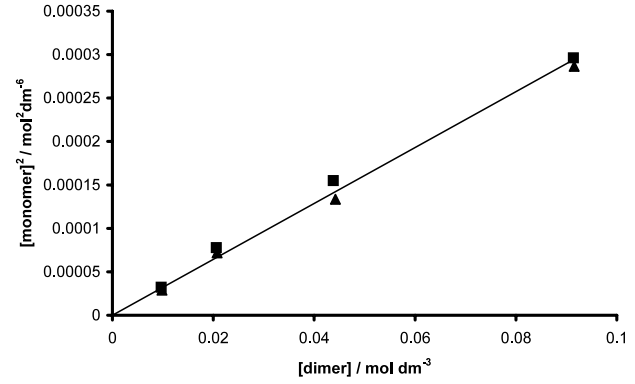

Fig. 2. Plot of concentration (monomer)^2 vs. concentration (dimer), ^{11}B-data (▲) and ^{1}H-data (■).

2.3. Variable temperature NMR study

A solution of dimesitylborane in deuterated toluene was examined by variable temperature NMR spectroscopy from 203 to 333 K (Fig. 3). As temperature increases, the proportion of monomer increases from ca. zero at 253 K to ca. 50% at 333 K. The line width in the $^{11}B\{^1H\}$-NMR spectrum was also strongly temperature dependent, decreasing from 3000 Hz (dimer, 203 K) to 640 Hz (dimer, 333 K). The monomer/dimer peaks showed no evidence of coalescence even at 333 K, indicating a very slow rate of exchange. A van't Hoff plot of $-\ln[K_{diss}(T)]$ vs. $1/T$ (Fig. 4) was used to determine the enthalpy of dissociation, ΔH, which was found to be 70 kJ mol^{-1}. The value of ΔS for dissociation (from a plot of $\Delta G/T$ vs. $1/T$) was

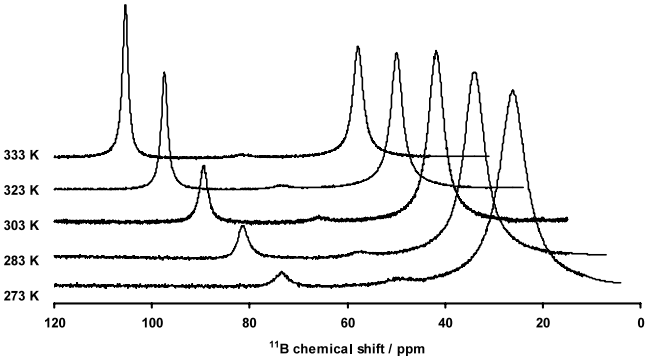

Fig. 3. Effect of varying temperature on the $^{11}B\{^1H\}$ spectrum of dimesitylborane.

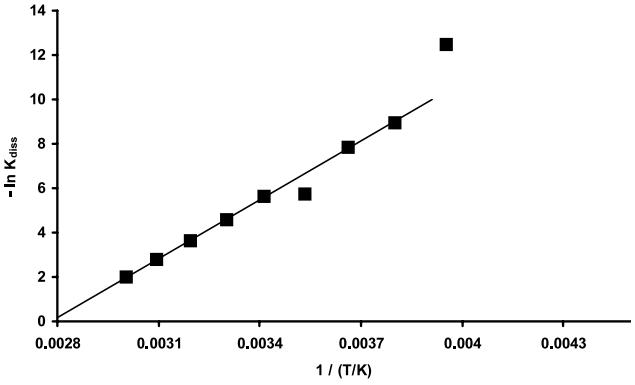

Fig. 4. van't Hoff plot showing variation of K_{diss} with temperature.

calculated to be 212 J K^{-1} mol^{-1}, similar to that found for 10-TMS-9-BBD-H (-198 J K^{-1} mol^{-1} for association of monomer) [16], though it should be noted that the relatively small temperature range may lead to correspondingly large errors in the calculation.

2.4. Neutron and X-ray crystallography

The solid-state structure of dimesitylborane dimer was determined by single crystal neutron diffraction at 20 K and X-ray diffraction at 120 K (Fig. 5). Important geometrical parameters are listed in Table 2. The B–H bond length determined by X-ray diffraction is significantly shorter than the length determined from neutron diffraction, consistent with the errors associated with locating the hydrogen atom by X-ray diffraction [23]. This is also apparent from the reduced B–H–B angle and the larger e.s.d.s in the X-ray data, and results in a

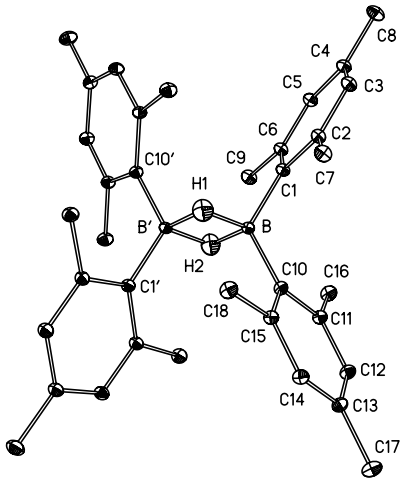

Fig. 5. ORTEP diagram of the molecular structure of $[Mes_2BH]_2$ (neutron data, 50% thermal ellipsoids) with all hydrogen atoms except the bridging hydrogens omitted for clarity. Bridging hydrogens are also represented by 50% thermal ellipsoids.

Table 2
Selected bond lengths and angles for the borane dimers $R_4B_2H_2$ by X-ray (R = Mes), neutron (R = Mes) and electron diffraction (R = Me, H) methods

$R_4B_2H_6$	R = Mes X-ray	R = Mes Neutron	R = Me Electron [33]	R = H Electron [34]
B–H (Å)	1.280(15)	1.340(2)	1.36(4)	1.339(4)
	1.288(16)	1.342(2)		
B···B (Å)	1.856(3)	1.855(2)	1.84(1)	1.775(4)
B–C (Å)	1.5959(19)	1.5959(13)	1.590(3)	
	1.5972(19)	1.6000(14)		
B–H–B (°)	93	87.7	85	83
H–B–H (°)	87.5(10)	92.46(14)	95(3)	97.0(3)
C–B–C (°)	123.43(11)	123.70(8)	120.0(13)	

contraction of the apparent B_2H_2 unit when determined by X-ray diffraction. This contraction of the B_2H_2 unit is also evident in X-ray crystal structures determined for related diborane (6) derivatives [15,17,24–32]. Geometrical values concerning the heavy atoms in the dimesitylborane dimer are within experimental error for both the neutron and X-ray structures. The B_2H_2 system in dimesitylborane is very close to D_{2h} symmetry, although only the twofold rotational axis through H1 and H2 is crystallographically imposed.

The location of hydrogens determined by gas-phase electron diffraction is considered to be accurate, and several diboranes [33–35] have been studied by this technique. Values for tetramethyldiborane ($Me_4B_2H_2$) and diborane (6) (B_2H_6) are included in Table 2 for comparison [33,34]. Although data are limited, there is an apparent trend in the structural parameters of the B_2H_2 unit on going from the bulky mesityl groups, to the less bulky methyl groups and finally, to hydrogens as the terminal groups, with the B···B distances becoming shorter and the H–B–H angles becoming larger. An interesting point in this series is that the B–H bond lengths remain largely unchanged.

A search of the Cambridge Structural Database reveals that forty structures of compounds containing boron have been solved using neutron diffraction. Of these, the majority are salts containing anions such as BF_4^- or BPh_4^-. Of the remaining compounds, twelve contain B–H bonds [36–44] including only three that contain B–H–B bridging bonds such as those occurring in the dimesitylborane dimer. Decaborane [45] exhibits a range of bridging B–H distances from 1.321 to 1.354 Å. In contrast, the B–H–B bridge in the compound [8-dimethylamino-1-(dimethylammonio)naphthalene]$^+$ [10,11-μ-H-7,8-dicarba-nido-undecaborate]$^-$ is unsymmetric, with a short bond length of 1.253 Å and a significantly longer bond of 1.469 Å [22]. In the heptahydroborate anion $[H_3B–H–BH_3]^-$ [46], the B–H–B is also unsymmetric, with rather short bond lengths of 1.324 and 1.216 Å. From this limited data set, it appears that the symmetric dimesitylborane dimer has bridging B–H bond distances that lie close to the midpoint of the range of values exhibited by B–H–B bridged compounds.

2.5. Computational studies

While the fully optimized geometry of the dimesitylborane dimer at the computationally intensive MP2/6-31G* level of theory is desirable for comparison with our experimental data, it could not be achieved due to computing limitations. Nevertheless, the optimized geometry of the dimer at the HF/6-31G* level is in fairly good agreement with the observed structural data. Calculated (GIAO) boron NMR shifts generated from the HF/6-31G* optimized geometries of the dimesitylborane monomer and dimer are 68.7 and 25.3 ppm in agreement with observed shifts of 73.3 and 25.9 ppm in aromatic solvents and 65.1 and 22.9 ppm in THF.

Unlike the dimesitylborane dimer, we were able to carry out MP2/6-31G* geometry optimizations of the dimesitylborane monomer and the related dimesitylfluoroborane. Selected geometric parameters for these compounds are listed in Table 3 and the fully optimized geometry of the monomer is shown in Fig. 6. Comparison of the optimized geometry of the dimesitylborane monomer with the structures of dimesitylfluoroborane (by optimized geometry and by X-ray diffraction [47]) and ditripylborane (by X-ray diffraction [17]) in Table 3 reveals a very good agreement between the optimized and X-ray geometries of the fluoroborane and that there is little difference in the geometry around the boron atom in all cases. The geometries are dominated by the steric effects of the mesityl groups rather than electronic or steric effects from the similarly sized fluorine or hydrogen atoms. Replacing a mesityl group with the

Table 3
Selected bond lengths and angles for the MP2/6-31G* optimized dimesitylborane monomer and dimesitylfluoroborane and for the structures of dimesitylfluoroborane and ditripylborane solved by X-ray diffraction

	Mes_2BH Calc	Mes_2BF Calc	Mes_2BF X-ray [47]	$Trip_2BH$ X-ray [17]
B–X (Å)	1.202	1.354	1.339(2)	1.13(4)
B–C (Å)	1.557	1.563	1.568(2)	1.564(6)
			1.570(2)	1.570(6)
C–B–C (°)	124.21	125.66	125.39(14)	128.0(4)
C–B–X (°)	117.90	117.17	116.82(14)	116(2)
	117.88		117.79(14)	116(2)

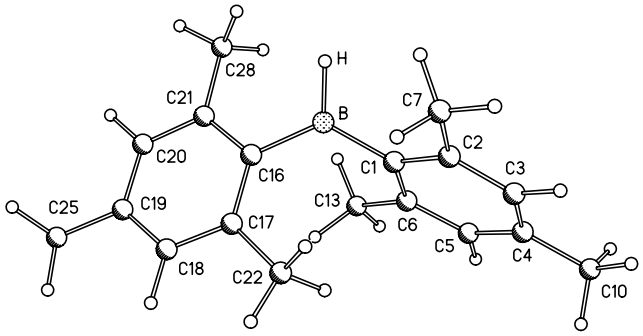

Fig. 6. Ball and stick diagram of the optimized geometry of Mes_2BH at the MP2/6-31G* level.

bulkier tripyl group causes an increase in the C–B–C angle due to even greater steric congestion. The experimental value of the B–H bond length in the ditripylborane is, as expected for X-ray diffraction, shorter than that for the optimized geometry of the dimesitylborane monomer. The ^{11}B-NMR shift computed (at the GIAO-B3LYP/6-311G* level) for the MP2/6-31G* optimized geometry of the dimesitylborane monomer is 70.6 ppm, confirming this geometry to be present in solution.

Table 4 lists the binding energies for a selection of boranes that are either known in the monomeric form or commonly used in hydroboration. These were calculated from the energies of monomeric and dimeric species for which geometries were optimized at the HF/6-31G* level [48]. The binding energy of the dimesitylborane dimer was computed to be -79 kJ mol^{-1}, which indicates the dimesitylborane monomer to be the more stable form thermodynamically in the gas-phase. It is stressed here that this value is only useful for comparing with related boranes since a low level of theory was used [48]. The trends in the binding energies are in broad agreement with the monomeric and dimeric species reported experimentally [15–17,26,27,33,34,49]. It is clear from Table 4 that the trend towards monomeric species on going from diphenylborane, dimesitylborane to ditripylborane is due to steric factors.

3. Conclusions

We show here by NMR spectroscopy that the dimesitylborane monomer exists in equilibrium with the known dimesitylborane dimer. The presence of relatively large amounts of monomer in dimesitylborane solutions can be attributed mainly to steric factors, with the change from four to three-coordination on forming the monomer relieving congestion. The low reactivity of dimesitylborane, despite the high proportion of monomer, may be due to steric bulk, inhibiting the formation of a π-complex with unsaturated substrates, or due to a labile complex with donor solvents such as THF. Neutron diffraction was carried out on a diborane (6) compound for the first time, providing a more accurate geometry of the BH_2B unit in the solid-state than could be achieved by X-ray diffraction. By *ab initio* computations, the geometry of the dimesitylborane monomer was optimized at the MP2/6-31G* level and confirmed by the computed boron NMR shift. The trend in the binding energies calculated between the monomer and dimer in selected boranes is in good agreement with their known tendencies to exist as monomeric and/or dimeric species.

Table 4
Total and binding energies for selected boranes at the HF/6-31G* level of theory

R	R_2BH (au)	$R_4B_2H_2$ (au)	Binding energy (kJ mol^{-1})	Known species
Tripyl	−1188.12265	dissociates	–	Monomer
R_2 = cat	−404.62598	dissociates	–	Monomer
Thexyl	−494.79999	dissociates	–	Monomer
R_2BH = 9-TMS-10-BBD	−782.59496	−1565.15523	−91.06	Dimer/monomer
Mesityl	−719.72702	−1439.42378	−79.42	Dimer/monomer
Phenyl	−485.52413	−971.03316	−39.62	Not known
C_6F_5	−1473.96407	−2947.92446	−9.68	Dimer/monomer
Methyl	−104.49136	−208.99327	27.70	Dimer
R_2BH = 9-BBN	−336.35384	−672.72162	36.59	Dimer
H	−26.39001	−52.812401	85.01	Dimer

A positive sign in the binding energy indicates that the dimer is lower in energy than the separated monomers.

4. Experimental

4.1. General

Dimesitylborane was synthesised by the reduction of dimesitylfluoroborane with $LiAlH_4$ according to a published procedure [2] and recrystallised from THF/diethyl ether. NMR solvents were dried and distilled from sodium-benzophenone prior to use, and solutions were made up in an Innovative Technology Inc. nitrogen-filled glovebox. NMR spectra were acquired on a Varian Unity Inova 500 MHz spectrometer. Proton spectra were recorded at 500 MHz and referenced to tetramethylsilane. Boron spectra were recorded at 160 MHz and referenced to $BF_3{\cdot}OEt_2$.

4.2. Computational methods

All *ab initio* computations were carried out with the Gaussian 98 package [50]. The structures of the dimesitylborane dimer and monomer were optimized at the HF/6-31G* level with no symmetry constraints. Frequency calculations were computed on these optimized geometries at the HF/6-31G* level for imaginary frequencies. Optimization of the HF/6-31G* geometry for the monomer was then carried out at the computationally intensive MP2/6-31G* level of theory. Theoretical ^{11}B chemical shifts were referenced to B_2H_6 (16.6 ppm) [51] and converted to the usual $BF_3{\cdot}OEt_2$ scale: $\delta(^{11}B) = 123.4 - \sigma(^{11}B)$ at the RHF/6-31G*//RHF/6-31G* level and $\delta(^{11}B) = 102.83 - \sigma(^{11}B)$ at GIAO-B3LYP/6-311G*//MP2/6-31G*.

4.3. Neutron structure determination

A clear rod shaped crystal of dimensions $0.9 \times 1.4 \times 5.2$ mm^3 was glued with Kwikfill to a 1 mm V pin, and cooled slowly to 20 K using an Air Products 201 Helium Displex [52] cryorefrigerator on the D19 instrument [53] at the ILL (equipped with both a $4^\circ \times 64^\circ$ 'banana' detector and a $20^\circ \times 20^\circ$ square detector). Reflections were collected on both detectors quasi-simultaneously using equatorial and normal beam geometry, and scaled together empirically using common reflections. Three standard reflections showed no change in intensity during the data collection. Reflections were integrated using the 'RETREAT' software [54]. Neutron structure refinement was carried out using SHELXL-97 [55]. Neutron coherent scattering lengths were taken from Ref. [56]. The initial difference Fourier map showed clearly the positions of the ordered hydrogen atoms, though the presence of residual density in the difference map around the methyl group of C(16), coupled with very large anisotropic displacement parameters, led to a disordered model for this group. Full anisotropic refinement for all atoms was then carried out.

Crystal data for dimesitylborane: $C_{36}H_{46}B_2$. $M = 500.00$, pale yellow block, 6.25 mm^3 monoclinic, space group $P2/n$ (No. 10), $a = 12.2778(8)$, $b = 7.7353(6)$, $c = 16.5979(2)$ Å, $\beta = 109.836^\circ$, $V = 1482.81(18)$ Å^3, $Z = 2$, $D_{calc} = 1.120$ Mg m^{-3}, $F_{0\,0\,0} = 156$, ILL D19, neutron radiation, $\lambda = 1.3186(1)$ Å, $T = 20(2)$ K, $2\theta_{max} = 132.28^\circ$, 10 868 reflections collected, 3342 unique ($R_{int} = 0.0391$). Final GoF = 1.134, $R_1 = 0.0354$, $wR_2 = 0.0833$, R indices based on 3078 reflections with $I > 2\sigma(I)$ (refinement on F^2), 409 parameters, 0 restraints. Absorption corrections ($\mu = 4.44$ cm^{-1}) were applied with the program D19ABS, based on the ILL version of the CCSL system [57].

4.4. X-ray structure determination

A clear block shaped crystal of dimensions $0.3 \times 0.2 \times 0.12$ mm^3 was oil mounted onto a hair and flash cooled to 120 K under nitrogen gas flow, Oxford Cryosytems Cryostream [58]. 16 175 reflections ($2.58 < \theta < 28.46^\circ$) were collected on a Brucker SMART-CCD 6K diffractometer [59,60] (ω-scans, 0.3° frame^{-1}) yielding 3817 unique data. The structure was solved by direct methods and refined by full matrix least-squares based on F^2 for all data using SHELXL-97 [55] software. All non-hydrogen atom were refined with anisotropic displacement factors, hydrogen atoms were placed geometrically at calculated positions and refined with a model. Though the presence of residual electron density in the difference map around the methyl groups of C(13), C(14), C(15) and C(16), a disordered model for these groups was employed. Final GoF = 1.042, $R_1 = 0.0501$, $wR_2 = 0.1441$, R indices based on 2855 reflections with $I > 4\sigma(I)$ (192 parameters).

$a = 12.2566(6)$, $b = 7.7598(4)$, $c = 16.7075(9)$ Å, $\beta = 109.5960(10)^\circ$, $V = 1496.99(13)$ Å^3 monoclinic, space group $P2/n$ (No. 10), Mo–K_α, $\lambda = 0.71073$ Å, $D_{calc} = 1.110$ Mg m^{-3}.

5. Supplementary material

Neutron and X-ray crystallographic data for the dimesitylborane dimer have been deposited with the Cambridge Crystallographic Data Centre, Dep. No. CCDC 205851 (neutron data), and 205852 (X-ray data). Copies of this information may be obtained free of charge from The Director, CCDC, 12 Union Road, Cambridge CB2 1EZ, UK (Fax: +44-1223-336033; e-mail: deposit@ccdc.cam.ac.uk or www: http://www.ccdc.cam.ac.uk).

Acknowledgements

We thank the EPSRC for postgraduate studentships (C.D.E. and P.S.S.), an Advanced Research Fellowship (M.A.F.) and a Senior Research Fellowship (J.A.K.H.), and we thank Mr I. McKeag and Dr A.M. Kenwright for assistance in acquiring the NMR spectra.

References

[1] J. Hooz, S. Akiyama, F.J. Cedar, M.J. Bennet, R.M. Tuggle, J. Am. Chem. Soc. 96 (1974) 274.
[2] A. Pelter, S. Singaram, H.C. Brown, Tetrahedron Lett. 24 (1983) 1433.
[3] Z. Yuan, N.J. Taylor, R. Ramachandran, T.B. Marder, Appl. Organomet. Chem. 10 (1996) 305.
[4] Z. Yuan, N.J. Taylor, T.B. Marder, I.D. Williams, S.K. Kurtz, L.T. Cheng, J. Chem. Soc. Chem. Commun. (1990) 1489.
[5] N. Matsumi, K. Naka, Y. Chujo, J. Am. Chem. Soc. 120 (1998) 5112.
[6] N. Matsumi, M. Miyata, Y. Chujo, Macromolecules 32 (1999) 4467.
[7] M.E. Glagowski, J.L.R. Williams, J. Organomet. Chem. 216 (1981) 1.
[8] J. Fiedler, S. Zalis, A. Klein, F.M. Hornung, W. Kaim, Inorg. Chem. 35 (1996) 3039.
[9] M. Lequan, R.M. Lequan, K.C. Ching, J. Mater. Chem. 2 (1992) 719.
[10] M. Kinoshita, Y. Shirota, Chem. Lett. (2001) 614.
[11] S. Yamaguchi, S. Akiyama, K. Tamao, Org. Lett. 2 (2000) 4129.
[12] Z. Liu, Q. Fang, D. Wang, G. Xue, W. Yu, Z. Shao, M. Jiang, Chem. Commun. (2002) 2900.
[13] (a) C.D. Entwistle, T.B. Marder, Angew. Chem. Int. Ed. Eng. 41 (2002) 2927;
(b) Z. Yuan, J.C. Collings, N.J. Taylor, T.B. Marder, C. Jardin, J.-F. Halet, J. Solid State Chem. 154 (2000) 5.
[14] J. Chandrasekharan, H.C. Brown, J. Org. Chem. 50 (1985) 518.
[15] D.J. Parks, W.E. Piers, G.P.A. Yap, Organometallics 17 (1998) 5492.
[16] J.A. Soderquist, K. Matos, C.H. Burgos, C. Lai, J. Vacquer, J.R. Medina, In: M.G. Davidson, A.K. Hughes, T.B. Marder, K. Wade (Eds.), Contemporary Boron Chemistry, Special Publication No. 253, The Royal Society of Chemistry, Cambridge (2000) p. 472.
[17] R.A. Bartlett, H.V. Rasika Dias, M.M. Olmstead, P.P. Power, K.J. Weese, Organometallics 9 (1990) 146.
[18] E. Negishi, J.J. Katz, H.C. Brown, J. Am. Chem. Soc. 94 (1972) 4025.
[19] S. Aldridge, R.J. Calder, A. Rossin, A.A. Dickinson, D.J. Willock, C. Jones, D.J. Evans, J.W. Steed, E.M. Light, S.J. Coles, M.B. Hursthouse, J. Chem. Soc. Dalton Trans. (2002) 2020.
[20] C.F. Lane, G.W. Kabalka, Tetrahedron 32 (1976) 981.
[21] N.N. Ho, R. Bau, C. Plecnik, S.G. Shore, X. Wang, A.J. Schultz, J. Organomet. Chem. 654 (2002) 216.
[22] M.A. Fox, A.E. Goeta, J.A.K. Howard, A.K. Hughes, A.L. Johnson, D.A. Keen, K. Wade, C.C. Wilson, Inorg. Chem. 40 (2001) 173.
[23] D.S. Jones, W.N. Lipscomb, Acta Crystallogr. A 26 (1970) 196.
[24] H.W. Smith, W.N. Lipscomb, J. Chem. Phys. 43 (1965) 1060.
[25] J. Liu, E.A. Meyers, S.G. Shore, Inorg. Chem. 37 (1998) 496.
[26] D.J. Brauer, C. Krüger, Acta Crystallogr. B 29 (1973) 1684.
[27] R. Köster, H.G. Willemsen, Liebigs Ann. Chem. (1974) 1843.
[28] S.S. Al-Juaid, C. Eaborn, P.B. Hitchcock, K.K. Kundu, M.E. Molla, J.D. Smith, J. Organomet. Chem. 385 (1990) 13.
[29] P. Paetzold, L. Geret, R. Boese, J. Organomet. Chem. 385 (1990) 1.
[30] M. Yalpani, R. Boese, R. Köster, Chem. Ber. 120 (1987) 607.
[31] H. Wadepohl, U. Arnold, H. Pritzkow, Angew. Chem. Int. Ed. Engl. 36 (1997) 974.
[32] T. Mennekes, P. Paetzold, R. Boese, Angew. Chem. Int. Ed. Engl. 29 (1990) 899.
[33] B.L. Carroll, L.S. Bartell, J. Am. Chem. Soc. 42 (1965) 1135.
[34] B.L. Carroll, L.S. Bartell, Inorg. Chem. 7 (1968) 219.
[35] L. Hedberg, K. Hedberg, D. Kohler, D.M. Ritter, W. Schomaker, J. Am. Chem. Soc. 102 (1980) 3430.
[36] E.J. Corey, N.J. Cooper, W.M. Canning, W.N. Lipscomp, T.F. Koetzle, Inorg. Chem. 21 (1982) 192.
[37] S.H. Lawrence, S.G. Shore, T.F. Koetzle, J.C. Huffman, C.-Y. Wei, R. Bau, Inorg. Chem. 24 (1985) 3171.
[38] W.T. Klooster, T.F. Koetzle, P.E.M. Siegbahn, T.B. Richardson, R.H. Crabtree, J. Am. Chem. Soc. 121 (1999) 6337.
[39] E.R. Bernstein, W.C. Hamilton, T.A. Keiderling, S.J. La Placa, S.J. Lippard, J.J. Mayerele, Inorg. Chem. 11 (1972) 3009.
[40] R.W. Broach, I.-S. Cheung, T.J. Marks, J.M. Williams, Inorg. Chem. 22 (1983) 1081.
[41] S.A. Kahn, J.H. Morris, M. Harman, M.B. Hursthouse, J. Chem. Soc. Dalton Trans. (1992) 119.
[42] P.L. Johnson, S.A. Cohen, T.J. Marks, J.M. Williams, J. Am. Chem. Soc. 100 (1978) 2709.
[43] F. Takusagawa, A. Fumagalli, T.F. Koetzle, S.G. Shore, T. Schmitikons, A.V. Fratini, K.W. Morse, C.-Y. Wei, R. Bau, J. Am. Chem. Soc. 103 (1981) 5165.
[44] P. Singh, M. Zottola, S.Q. Huang, B.R. Shaw, L.G. Pedersen, Acta Crystallogr. C 52 (1996) 52.
[45] R. Brill, H. Dietrich, H. Dierks, Acta Crystallogr. B 27 (1971) 2003.
[46] S.I. Kahn, M.Y. Chiang, R. Bau, T.F. Koetzle, S.G. Shore, S.H. Lawrence, J. Chem. Soc. Dalton Trans. (1986) 1753.
[47] S.M. Cornet, K.B. Dillon, C.D. Entwistle, M.A. Fox, A.E. Goeta, T.B. Marder, A.L. Thompson, J. Organomet. Chem., in preparation.
[48] D.J. DeFrees, K. Raghavachari, H.B. Schlegel, J.A. Pople, P.v.R. Schleyer, J. Phys. Chem. 91 (1987) 1857.
[49] R. Koster, G. Benedikt, Angew. Chem. Int. Ed. Engl. 2 (1963) 323.
[50] Gaussian 98, Revision A.9, M.J. Frisch, G.W. Trucks, H.B. Schlegel, G.E. Scuseria, M.A. Robb, J.R. Cheeseman, V.G. Zakrzewski, J.A. Montgomery Jr., R.E. Stratmann, J.C. Burant, S. Dapprich, J.M. Millam, A.D. Daniels, K.N. Kudin, M.C. Strain, O. Farkas, J. Tomasi, V. Barone, M. Cossi, R. Cammi, B. Mennucci, C. Pomelli, C. Adamo, S. Clifford, J. Ochterski, G.A. Petersson, P.Y. Ayala, Q. Cui, K. Morokuma, D.K. Malick, A.D. Rabuck, K. Raghavachari, J.B. Foresman, J. Cioslowski, J.V. Ortiz, A.G. Baboul, B.B. Stefanov, G. Liu, A. Liashenko, P. Piskorz, I. Komaromi, R. Gomperts, R.L. Martin, D.J. Fox, T. Keith, M.A. Al-Laham, C.Y. Peng, A. Nanayakkara, M. Challacombe, P.M.W. Gill, B. Johnson, W. Chen, M.W. Wong, J.L. Andres, C. Gonzalez, M. Head-Gordon, E.S. Replogle, J.A. Pople, Gaussian, Inc., Pittsburgh PA, 1998.
[51] T.P. Onak, H.L. Landesman, R.E. Williams, J. Phys. Chem. 63 (1959) 1533.
[52] J.M. Archer, M.S. Lehmann, J. Appl. Cryst. 21 (1986) 471.
[53] M. Thomas, R.F.D. Stansfield, M. Berneron, A. Filhol, G. Greenwood, J. Jacobe, D. Feltin, S.A. Mason, in: P. Convert, J.B. Forsyth (Eds.), Position-Sensitive Detection of Thermal Neutrons, Academic Press, London, 1983, p. 344.
[54] C. Wilkinson, H.W. Khamis, R.F.D. Stansfield, G.J. McIntyre, J. Appl. Cryst. 21 (1988) 471.
[55] G.M. Sheldrick, SHELXL-97, University of Göttingen, 1997.

[56] V.F. Sears, Neutron News 3 (1992) 26.
[57] J.C. Matthewman, P. Thompson, P.J. Brown, J. Appl. Cryst. 15 (1982) 167.
[58] J. Cosier, A.M. Glazer, J. Appl. Cryst. 19 (1986) 105.
[59] Bruker SMART-V5.625. Data Collection Software. Siemens Analytical X-ray Instruments Inc., Madison, Wisconsin, USA.
[60] Bruker SAINT-V6.28A. Data Reduction Software. Siemens Analytical X-ray Instruments Inc., Madison, Wisconsin, USA.